IEEE Photonics Journal
An IEEE Photonics Society Publication

Open Access

Direct Design of Thin and High-Quality Direct-Lit LED Backlight Systems

Volume 13, Number 2, April 2021

Zhanghao Ding
Yingli Liu
Yaoguang Ma
Zhenrong Zheng
Min Wang
Ping Zeng
Jun She
Rengmao Wu

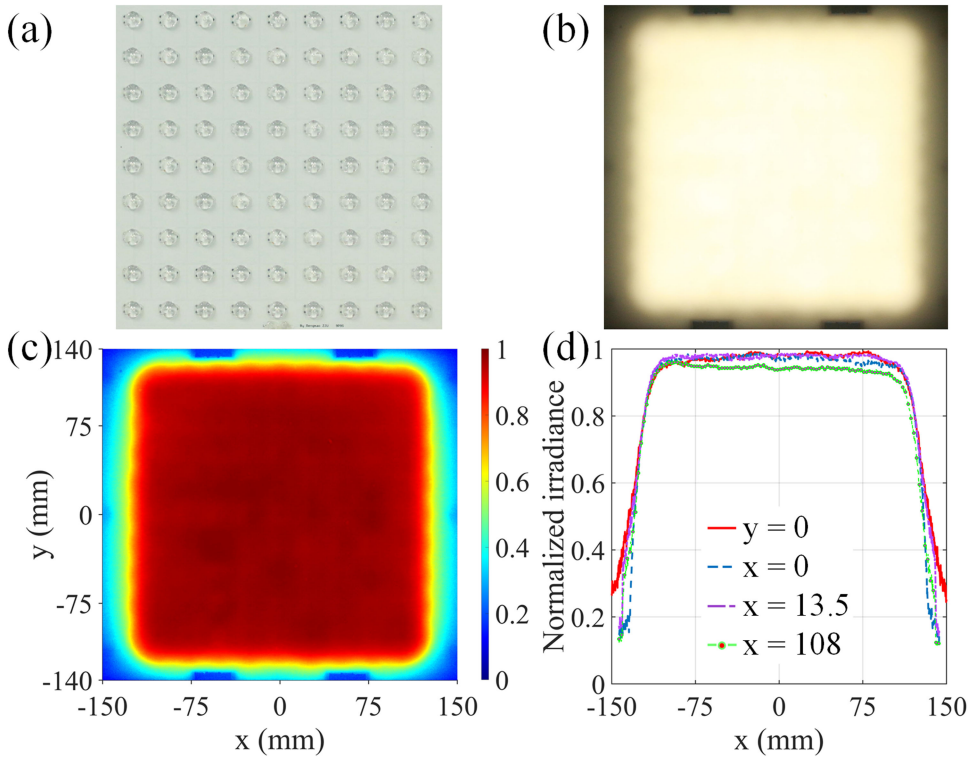

DOI: 10.1109/JPHOT.2021.3068746

Direct Design of Thin and High-Quality Direct-Lit LED Backlight Systems

Zhanghao Ding,[1] **Yingli Liu**,[1] **Yaoguang Ma**,[1] **Zhenrong Zheng**,[1] **Min Wang**,[2] **Ping Zeng**,[3] **Jun She**,[4] **and Rengmao Wu**[1]

[1]State Key Laboratory of Modern Optical Instrumentation, College of Optical Science and Engineering, Zhejiang University, Hangzhou 310027, China
[2]Nanchang Opto-Electric R&D Institute Co., Ltd., Nanchang 330096, China
[3]CECEP Latticelighting Co., Ltd., Nanchang 330096, China
[4]Yejia Optical Technology (Guangdong) Corporation, Dongguan 523711, China

DOI:10.1109/JPHOT.2021.3068746

Manuscript received February 23, 2021; revised March 19, 2021; accepted March 22, 2021. Date of publication March 24, 2021; date of current version April 12, 2021. This work was supported by the National Natural Science Foundation of China (NSFC) under Grants 11804299, 62022071, 12074338 and "the Fundamental Research Funds for the Central Universities" +2018QNA5001. Corresponding author: Rengmao Wu (e-mail: wrengmao@zju.edu.cn).

Abstract: The direct-lit LED backlight is a key component in large-area LCD displays. The existing methods which rely on point source assumption and irradiance feedback are less effective in compact designs in near field, and designing thin and high-quality back-lit LED backlights still remains a challenging issue. In this paper, we develop a direct method for designing thin and high-quality back-lit LED backlight systems. The étendue of LED light sources is considered in the numerical calculation of the lens profiles without cumbersome Monte Carlo ray tracing, which allows us to obtain compact LED lighting modules and achieve accurate control of the near-field irradiance distribution of the backlight system. Two examples are presented to demonstrate the elegance of this method in designing thin and high-quality back-lit LED backlights.

Index Terms: Backlight system, Illumination design, LED array, Non-zero étendue.

1. Introduction

Light-emitting diode (LED) backlights endow liquid-crystal displays (LCDs) with a variety of advantages (e.g., wider color gamut, lower power consumption, less weight) over the traditional cold cathode fluorescent backlit LCDs [1]. LED LCDs have applied in a wide range of applications, covering LCD televisions, computer monitors, instrument panels, and indoor and outdoor signage. The direct-lit LED backlight, which generates high-quality large-scale uniform illumination by placing a set of LED lighting modules in a flat array behind the screen, is a key component in a large-area LCD display [2], [3], because the displayed image quality depends on the quality of the LED backlight and the thickness of the LCD display system is also strongly affected by the backlight thickness. According to the installation position of light sources, the backlight systems can be simply grouped into two types: edge-lit system which light sources arranged along the edges of the screen and direct-lit system which light sources organized directly behind the screen. While an edge-lit backlight system has a much thinner structure and a lower cost, a direct-lit backlight system has a much better performance of local dimming technique and its system size is unrestricted, thus the latter is more suitable for large-area LCD displays.

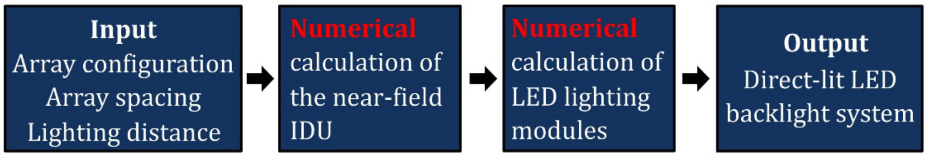

Fig. 1. The flow chart of the proposed direct method.

Due to the non-zero étendue of LED light sources, designing thin and high-quality direct-lit LED backlights becomes a challenging and rewarding issue. There are two typical scenarios for generating a direct-lit LED backlight. In the first scenario, a set of LED sources are embedded in a flat array at an optimized interval [4]. With a fixed lighting distance, the array spacing is fully governed by the irradiance distribution unit (IDU) produced by a single LED source. A smaller lighting distance means a smaller array spacing. Due to the typical cosine irradiance distribution of an LED source [4], a high package density cannot be avoided. From the aspect of cost control and system assembly, a smaller package density, which means a larger array spacing, is needed. In the second scenario, secondary lenses are employed to redistribute the light from LED sources to reduce the package density [5]–[11]. The use of secondary lenses allows us to generate an optimum IDU at a prescribed package density and lighting distance, which offers high degree of freedom for designing LED backlight. In this scenario, tailoring of the secondary lenses is a key point. Since an LED source has a certain size and angular extent, those designs which rely on zero étendue assumption becomes invalid when designing a thin LED backlight, in which the influence of the étendue of the LED source on the backlight performance cannot be ignored [5]–[7]. Feedback or optimization methods can be used to alleviate the performance deterioration caused by the étendue of the source to a certain extent [8]–[10]. Due to the nature of a feedback/optimization design, the system performance is strongly determined by the starting point, which is usually obtained by a zero-étendue algorithm [12-18]. It will be difficult to optimize a secondary lens in near field without a suitable starting point. Besides, the cumbersome Monte Carlo ray tracing is another major limitation of the feedback/optimization methods. Further, the feedback/optimization methods are less effective in compact designs [12]. To our knowledge, designing thin and high-quality direct-lit LED backlights is still not well addressed and faces many unresolved challenges.

In this paper, we develop a direct method for designing thin and high-quality back-lit LED backlight systems. The main contributions of this work are threefold: (1) the proposed method overcomes the limitations of the existing methods, achieving compact and high-performance systems, and stray rays are significantly reduced; (2) the proposed method can achieve precise control on light propagation in near field, which allows us to generate thin direct-lit backlights; (3) the backlight system is numerically calculated by the proposed method without cumbersome Monte Carlo ray tracing, which may open up a new avenue for designing direct-lit LED backlights. The rest of this paper is organized as follows. In Section II, the design principles of the proposed direct method will be introduced in detail, and the numerical calculation of the LED lighting modules which is a key point of the proposed method will also be presented. In Section III, an example will be presented to verify the effectiveness of the proposed method and elaborate analyses of this design will also be made in this section. After that, some characteristics of the proposed method will be discussed before we conclude our work in Section V.

2. Principles and Method

Fig. 1 gives the flow chart of the proposed method which includes two design phases. The purpose of the first phase is to find a target near-field IDU based on a given array configuration and array spacing. With this target near-field IDU, we then numerically calculate the LED lighting modules of the backlight system in the second phase instead of using any feedback or optimization designs. More details about the design process of this proposed direct method will be given in Fig. 1.

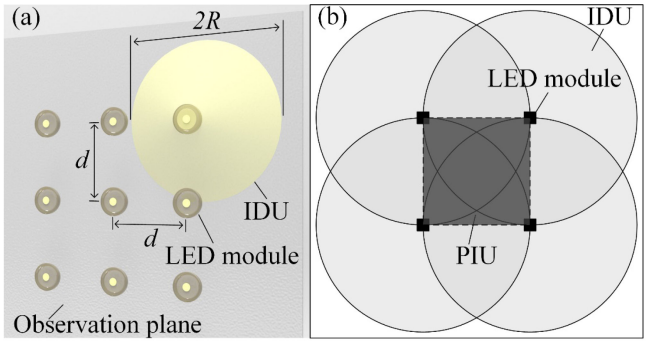

Fig. 2. (a) Geometrical layout of a direct-lit LED backlight system. *R* is the radius of the IDU. (b) Illustration of a PIU generated by a 2 × 2 array.

2.1 Numerical Calculation of the Near-Field IDU

The geometrical layout of the direct-lit LED backlight system is given in Fig. 2(a). The LED lighting module includes an LED source and a secondary lens which is an aspherical lens used to redistribute the spatial energy distribution of the LED source. The LED lighting modules are arranged along both the horizontal and vertical directions at an array spacing of *d*. It should be mentioned that the array configuration could also be triangular, circular, or linear [4], [5]. Application of the proposed method to a non-square configuration is straightforward, and will not be discussed here. In order to obtain a thin direct-lit backlight, we assume that the observation plane is placed so close to the LED source that the étendue of the LED source has a strong impact on tailoring of the secondary lens. Due to the rotational symmetry of the secondary lens, an even polynomial is used here to represent the IDU, which is given by

$$E(x, y) = \sum_{i=0}^{m} a_i \left(\sqrt{(x - x_0)^2 + (y - y_0)^2} \right)^i \tag{1}$$

where (x_0, y_0) are the coordinates of the center of the IDU on the observation plane; m is an even number; a_i ($i = 02, \ldots, m$) are the coefficients of the even polynomial, which are variables to be optimized in the first design phase. Since the LED sources are incoherent, the irradiance distribution produced by the backlight system on the observation plane is the sum of the near-field IDUs produced by the LED lighting modules. Superposition of the neighboring IDUs can yield a primary illumination unit (PIU). Accordingly, the large-scale illumination could be considered as a patchwork generated by translating the PIU along both the horizontal and vertical directions. Thus, the uniformity of the large-scale illumination is fully governed by that of the PIU. The more IDUs included in a primary illumination unit, the higher uniformity of the PIU could be. Obviously, the minimum number of the IDUs involved in the generation of a PIU equals four. In this case, the PIU is generated by a 2 × 2 array, which is defined by the centers of the four IDUs, as shown in Fig. 2(b). And, the LED array pitch is equal to the radius of IDU in a 2 × 2 array. The fractional RMS is employed here to represent the uniformity of the PIU, which is defined as

$$RMS = \sqrt{\frac{1}{num} \sum_{j=1}^{num} \left(\frac{E_j - \bar{E}}{\bar{E}} \right)^2} \tag{2}$$

where, *num* is the number of sample points defined on the PIU; E_j is the actual irradiance at the *j*-th sample point; $\bar{E}$ is the mean irradiance value of all sample points. A smaller value of RMS represents a higher uniformity of the PIU. It is of interest to mention that the Sparrow's criterion can also be used here to guarantee a high uniformity [7]. From Eqs. (1) and (2) we know that the uniformity of the PIU is a function of the coefficients a_i ($i = 0,2, \ldots, m$). Numerical optimization of

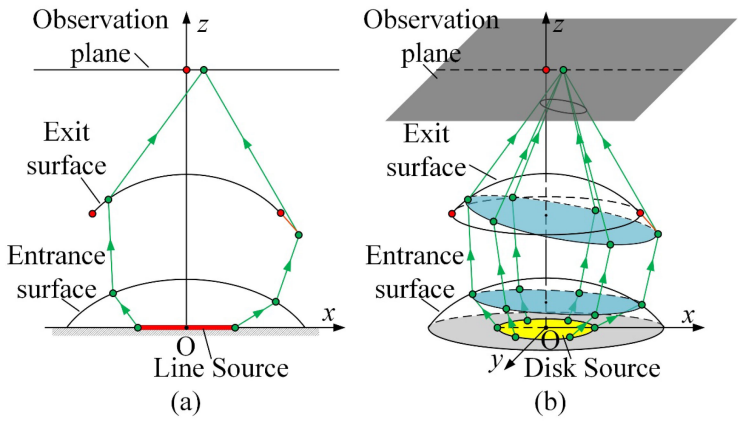

Fig. 3. Numerical calculation of the secondary lens. (a) An optimal entrance surface is numerical optimized in 2D geometry in the first step. (b) The exit surface is numerically calculated in 3D geometry in the second step.

the coefficients a_i is rather simple and fast. Both local and global optimization algorithms could be used. In this paper, the downhill simplex method which is a local algorithm is employed here to optimize the coefficients.

2.2 Numerical Calculation of LED Lighting Modules

Once we finalize the numerical calculation of the near-field IDU, we proceed to the second phase to design a secondary lens, by which the spatial energy distribution of the LED source is redistributed to produce the optimized near-field IDU. Due to the spatial and angular extent of an LED source, designing a compact aspherical lens to achieve an accurate control of the spatial energy distribution of the LED source in the near field is not a simple task. In our previous publication [18], we developed a direct method for designing aspherical lenses with prescribed near-field irradiance properties for extended Lambertian sources in 3D geometry. This direct method, which allows all the light rays from the extended source to be controlled well in a desired manner, can yield very compact lenses with high energy efficiency. Due to its unique characteristics, the direct method is used here to design the LED lighting module. The direct design of the secondary lens includes two steps, as illustrated in Fig.3. The purpose of the first step is to find an optimal entrance surface which could be a simple paraboloid surface or an aspherical surface. During the numerical optimization of the entrance surface, the profile of the exit surface is numerically calculated based on the basic relationship between the radiance of an incident beam and the near-field irradiance in 2D geometry which is given by

$$E_{2D} = \int L_{2D} \cos\varphi \, d\varphi \tag{3}$$

where, L_{2D} is the radiance of incident beam, E_{2D} is the 2D near-field irradiance, and $\cos\varphi$ is the direction cosine of the light beam in 2D geometry. When the light source is a Lambertian source, only the boundary rays of the light source are needed here because the radiance of the light beam is a constant. In the second step, the optimal entrance surface obtained from the first step is kept unchanged, and the exit surface of the lens is directly calculated numerically in 3D geometry in order to produce the optimized near-field IDU. Similarly, the exit surface is numerically calculated based on the basic relationship between the radiance of an incident beam and the near-field irradiance in 3D geometry which is given by

$$E_{3D} = \int L_{3D} \cos\theta \, d\omega \tag{4}$$

where L_{3D} denotes the radiance of incident beam in 3D geometry, E_{3D} denotes the target near-field irradiance in 3D geometry, $\cos\theta$ is the direction cosine of the light beam in 3D geometry, and ω is the solid angle subtended by the light beam. More details about these two design phases can be found in Ref. [19]. After construction of the secondary lens, the disk source employed in the second phase can be replaced by a square source with an almost unchanged output irradiance distribution, as long as the area of the square source is equal to that of the disk source [19]. After the LED lighting module is numerically calculated, the direct-lit LED backlight system is constructed by arranging the lighting modules along both the horizontal and vertical directions at a given array spacing.

3. Simulation and Experimental Verification

In the rest of this paper, two challenging design examples will be given to show the advantages and effectiveness of the proposed method. With regard to these designs, high precise control of light propagation is indispensable since the package density is considerably low and the lighting distance is too much short that the influence of the étendue of the source on the illumination cannot be ignored.

As an example, a direct-lit LED backlight system which includes 9 $\times$ 9 lighting modules is presented here. A 2 $\times$ 2 array is used here to generate the primary illumination unit. The size of the LED source equals 1.3 mm $\times$ 1.3 mm, which means the radius of the disk source used in the second design phase equals 0.7334 mm. The array spacing equals 27 mm, and the lighting distance between the source and the observation plane equals 8 mm. The lens material is Polycarbonate with refractive index of 1.584 at the wavelength of 546.1nm. We further assume that the radius of the IDU equals 27 mm, meaning that the PIU is generated by a 2 $\times$ 2 array. An 8th degree even polynomial is used here to represent the IDU, which means $m = 8$ in Eq. (1). After simple numerical optimization in the first design phase, we obtain the optimized near-field IDU, as shown in Fig. 4(a). Fig. 4(b) gives the irradiance distribution along the line y $=$ 0 mm, as denoted by the red solid line. Based on this target near-field IDU, the secondary lens is then numerically calculated in the second design phase. The lens model and lens profiles of the secondary lens are given in Fig. 4(c). From the lens profiles we know that the lens thickness equals 3.83 mm and the clear aperture of the lens equals 12.17 mm, which indicates that the secondary lens is very compact. The z-coordinate of the vertex of the entrance surface equals 1.46 mm. Then, we know that the ratio of the z-coordinate of the vertex of the entrance surface to the diagonal of the LED source equals 0.80, indicating that the étendue of the LED source has a very strong impact on tailoring of the secondary lens. The actual irradiance distribution produced by the lighting module is depicted in Fig. 4(b), which is denoted by the green dashed line. The fractional RMS is also employed here to quantify the difference between the actual IDU and the target. For a non-uniform design, $\bar{E}$ in Eq. (2) is the target irradiance at a sample point instead of the mean irradiance value. From Fig. 4(b) we have RMS $=$ 0.0157, showing a good agreement between the simulated IDU and the target. Then, the direct-lit backlight system is constructed by arranging the LED lighting modules into 9 rows and 9 columns at an array spacing of 27 mm. Since the PIU is produced by a 2 $\times$ 2 array, the size of the target uniform illumination region produced by the direct-lit LED backlight system equals 216 mm $\times$ 216 mm. Then, 162 million rays are traced to reduce statistical noise. The irradiance distribution produced by the backlight system on the observation plane is given in Fig. 4(d), the irradiance distributions along the lines x $=$ 0 mm and y $=$ 0 mm are depicted in Fig. 4(e). Fig. 4(d) tells us that RMS $=$ 0.0085, indicating a thin and high-performance direct-lit LED backlight system.

Fig. 4 gives the uniform irradiance distribution produced by the backlight system on an observation plane. In order to analyze the angular uniformity of the backlight system, the observation plane is replaced by a diffuser plate. The intensity distribution of the transmitted light beam is depicted in Fig. 5. From this figure we can see that a high angular uniformity can be guaranteed by use of a diffuser plate. Since assembly errors cannot be avoided when the secondary lenses are assembled on the printed circuit board, it is necessary to analyze the tolerance sensitivity of

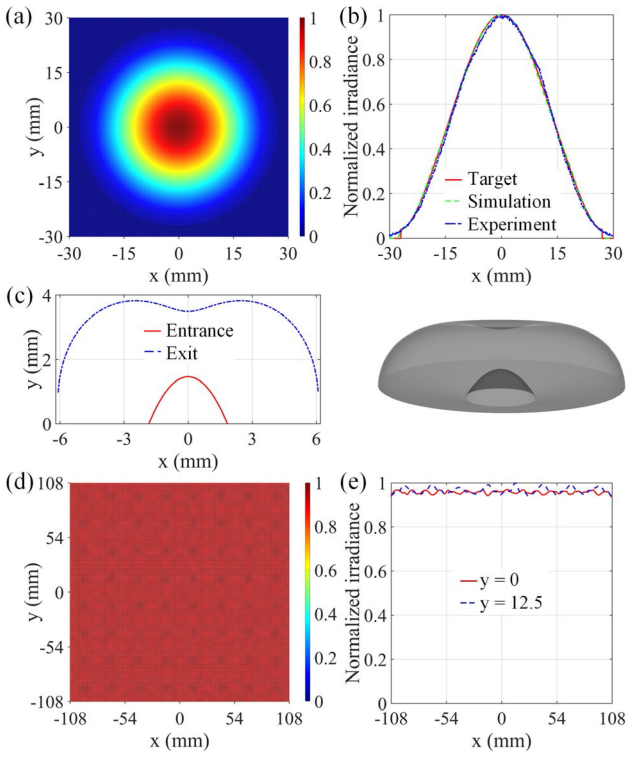

Fig. 4. Simulation verification: (a) the optimized near-field IDU ($a_0 = 15.3058$, $a_2 = -0.0475$, $a_4 = 6.6279\text{e-}05$, $a_6 = -6.6460\text{e-}08$, $a_8 = 3.7000\text{e-}11$); (b) the normalized irradiance distributions along the line y = 0 mm; (c) the profiles of the secondary lens; the entrance surface of the lens is a paraboloid surface which is defined by $z = -0.4322(x^2+y^2)+1.4639$; (d) the illumination pattern produced by the backlight system; (e) the normalized irradiance distributions along the lines y = 0 mm and y = 12.5 mm.

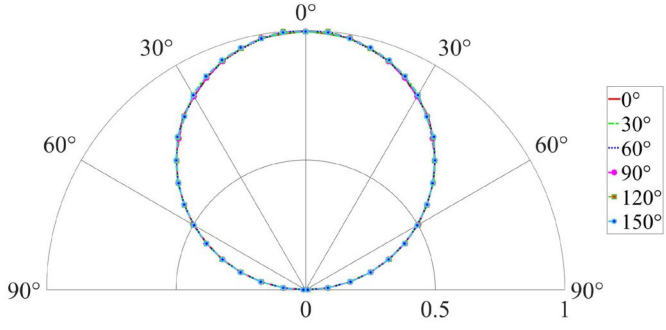

Fig. 5. Angular uniformity analysis of the backlight system. The observation plane (the receiver) is replaced by a diffuser plate and the intensity distribution of the transmitted light beam is recorded.

the backlight system. The positions of the LED sources are kept unchanged, and the lens array is shifted along the x- and z-axis directions, respectively. From Fig. 6 we can clearly see a high irradiance uniformity can still be guaranteed even if the displacement is increased to 0.1 mm.

The secondary lens is fabricated by injection molding. The prototype of the secondary lens is shown in Fig. 7(a), and the experimental setup is given in Fig. 7(b). A white LED source (LatticeShine CSP1313 2W) with size of 1.3 mm $\times$ 1.3 mm is used here [20]. The camera (Baumer VCXU-53C) is placed behind the observation plane to record the illumination pattern produced on the observation plane. The illumination pattern recorded in a darkroom environment is shown

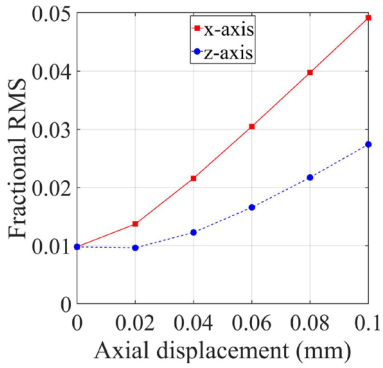

Fig. 6. Tolerance sensitivity analysis of the backlight system.

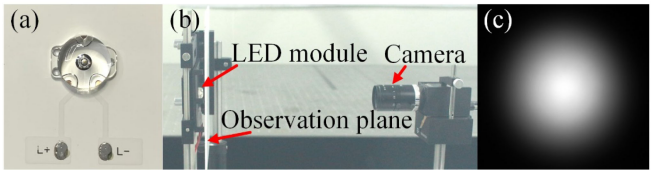

Fig. 7. Experimental verification of the LED lighting module: (a) the fabricated LED lighting module, (b) the experimental setup, and (c) the recorded IDU.

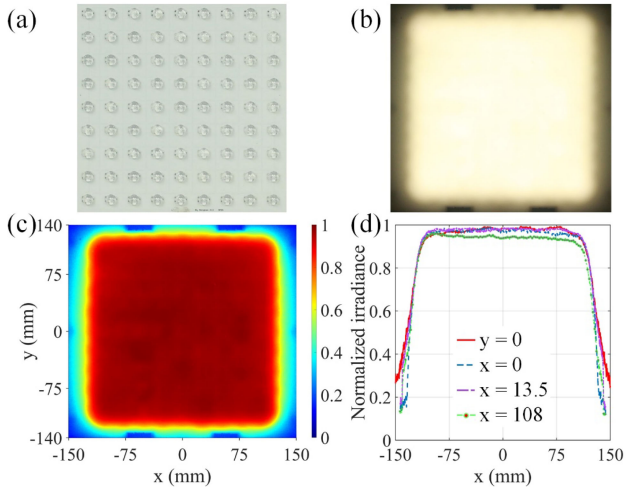

Fig. 8. Experimental verification of the backlight system: (a) the prototype of the direct-lit LED backlight system, (b) the recorded illumination pattern on the observation plane, (c) the normalized irradiance distribution of the illumination pattern, and (d) the irradiance distributions along the lines y = 0 mm, x = 0 mm, x = 13.5 mm, and x = 108 mm.

in Fig. 7(c) and the irradiance distribution along the line y = 0 mm is also plotted in Fig. 4(b), which is denoted by the blue dot-dashed line. From Fig. 4(b) we clearly see a good agreement between the actual irradiance and the target IDU. Fig. 8 shows the prototype of the direct-lit LED backlight system, in which the LED lighting modules are arranged on an aluminum printed circuit board. The illumination pattern on the observation plane recorded by the camera in a darkroom environment is given in Fig. 8(b). The normalized irradiance distribution of the illumination pattern is shown in Fig. 8(c). The irradiance distributions along the lines y = 0 mm, x = 0 mm, x = 13.5 mm,

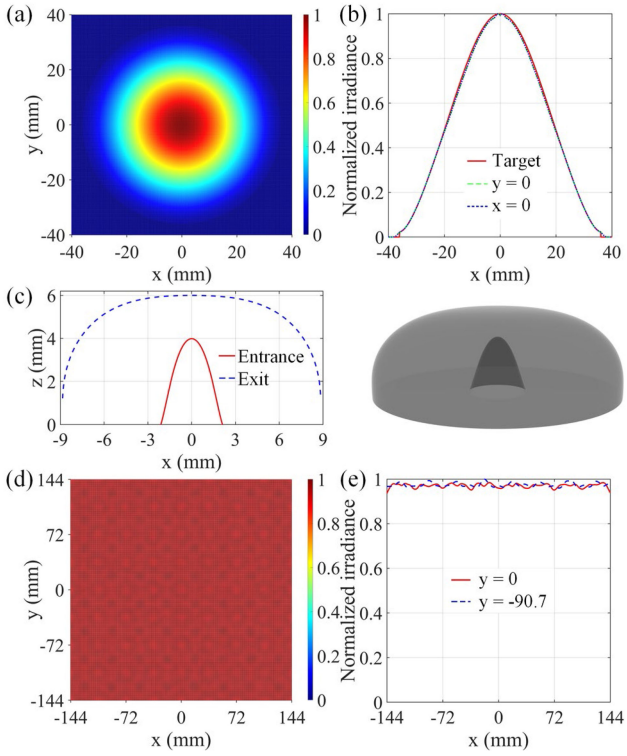

Fig. 9. Simulation verification in the second example: (a) the target near-field IDU ($a_0 = 12.7141$, $a_2 = -0.0222$, $a_4 = 1.7420\text{e-}05$, $a_6 = -9.8260\text{e-}09$, $a_8 = 3.0000\text{e-}12$) and (b) the irradiance distributions along the lines x = 0 mm and y = 0 mm; (c) the lens model and profiles of the secondary lens; the entrance surface of the secondary lens is given by $z = -8.2438\text{e-}05r^{10}+1.7344\text{e-}03r^8+6.8842\text{e-}03r^6-0.0537r^4\text{-}0.9121r^2+3.9841$; $r^2 = x^2+y^2$; (d) the large-scale uniform illumination produced by the backlight system; and (e) the normalized irradiance distributions along the lines y = 0 mm and y = −90.7 mm.

and x = 108 mm are depicted in Fig. 8(d). The fractional RMS is also used here to quantify the uniformity of the irradiance distribution. The fractional RMS equals 0.0132 within the target region {(x,y)|−108 mm ≤ x ≤ 108 mm, −108 mm ≤ y ≤ 108 mm}, showing the effectiveness of the proposed method. It is of great interest to mention that no total internal reflection (TIR) takes place at the exit surfaces of the secondary lenses due to the nature of the direct design that the étendue of the LED source is considered in tailoring of the lens profiles. That also means the stray rays caused by TIR are avoided. However, control of stray rays caused by TIR may be a big challenging in those feedback/optimization designs due to the limitations of feedback/optimization method [11].

4. Characteristics of the Proposed Direct Method

In the example given above, the ratio of the radius of the IDU to the lighting distance, which is usually called the distance-height ratio (DHR), equals 3.375. For a fixed lighting distance, a larger DHR means a larger array spacing (a smaller package density), and obviously a more challenging design. As mentioned above, the entrance surface of the secondary lens could be a simple paraboloid surface or an aspherical surface. Undoubtedly, an aspherical entrance surface offers more degrees of design freedom. We keep the lighting distance unchanged and increase the DHR to 4.5. That means the radius of the IDU is increased to 36 mm. A 10th degree even polynomial is used to represent the entrance surface of the secondary lens, and the other parameters remain unchanged. The optimized near-filed IDU is shown in Fig. 9(a), and the related irradiance distribution along the line y = 0 mm is given in Fig. 9(b), which is denoted by the red solid

line. The profiles of the secondary lens numerically calculated by the direct method are depicted in Fig. 9(c). The irradiance distributions produced by the LED lighting module are also given in Fig. 9(b). From Fig. 9(b) we can clearly see a good agreement between the actual irradiance and the target. Then, the direct-lit backlight system is constructed by arranging the LED lighting modules at an array spacing of 36 mm. Figs. 9(d) and 9(e) give the normalized irradiance distributions produced by the backlight system. The fractional RMS equals 0.0072 within the target region $\{(x, y)|-144\ \text{mm} \leq x \leq 144\ \text{mm}, -144\ \text{mm} \leq y \leq 144\ \text{mm}\}$, again showing the effectiveness of the proposed method. It is worth to mention that since the étendue of the LED source is considered in tailoring of the lens profiles, a smaller LED size which means a smaller étendue of the LED source can yield a smaller secondary lens and backlight thickness. Furthermore, the light source could also be a blue LED source, which means the proposed method could also be applied to quantum dot LED displays.

5. Conclusion

In this paper, we develop a direct method for designing thin and high-quality direct-lit LED backlight systems. Secondary lenses which need to be elaborately tailored are employed here to redistribute the light from LED sources, which offers high degree of freedom for designing LED backlight at a prescribed package density and lighting distance. The proposed direct method includes two design phases. The purpose of the first phase is to find a target near-field irradiance distribution unit based on a given array configuration and array spacing. With this target near-field irradiance distribution unit, we then numerically calculate the LED lighting modules of the backlight system in the second phase instead of using any feedback or optimization designs. The étendue of an LED source is considered in tailoring of the secondary lens which is numerically calculated to achieve precise control on light propagation in near field. The superiorities of the proposed direct design are demonstrated in the challenging designs through simulation and experimental tests. This method may open up an avenue for designing thin and high-quality direct-lit LED backlight systems, and may have great potential application in large-area LCD displays.

References

[1] K. H. Kim and J. K. Song, "Technical evolution of liquid crystal displays," *NPG Asia Mater.*, vol. 1, no. 1, pp. 29–36, Oct. 2009, doi: 10.1038/asiamat.2009.3.

[2] C. C. Sun, I. Moreno, S. H. Chung, W. T. Chen, C. T. Hsieh, and T. H. Yang, "Direct LED backlight for large area LCD TVs: Brightness analysis," in *Proc. SPIE*, 2007, pp. 666909-1–666909-10, doi: 10.1117/12.735508.

[3] H. W. Chen, J. H. Lee, B. Y. Lin, S. Chen, and S. T. Wu, "Liquid crystal display and organic light-emitting diode display: Present status and future perspectives," *Light Sci. Appl.*, vol. 7, no. 17168, pp. 1–13, Mar. 2018, doi: 10.1038/lsa.2017.168.

[4] I. Moreno, M. Avendaño-Alejo, and R. I. Tzonchev, "Designing light-emitting diode arrays for uniform near-field irradiance," *Appl. Opt.*, vol. 45, no. 10, pp. 2265–2272, Apr. 2006, doi: 10.1364/AO.45.002265.

[5] Z. Qin, K. Wang, F. Chen, X. Luo, and S. Liu, "Analysis of condition for uniform lighting generated by array of light emitting diodes with large view angle," *Opt. Exp.*, vol. 18, no. 16, pp. 17460–17476, Aug. 2010, doi: 10.1364/OE.18.017460.

[6] Z. Su, D. Xue, and Z. Ji, "Designing LED array for uniform illumination distribution by simulated annealing algorithm," *Opt. Exp.*, vol. 20, no. S6, pp. A843–A855, Nov. 2012, doi: 10.1364/OE.20.00A843.

[7] K. Wang, D. Wu, Z. Qin, F. Chen, X. Luo, and S. Liu, "New reversing design method for LED uniform illumination," *Opt. Exp.*, vol. 19, no. S4, pp. A830–A840, Jul. 2011, doi: 10.1364/OE.19.00A830.

[8] R. Wu, Z. Zheng, H. Li, and X. Liu, "Optimization design of irradiance array for LED uniform rectangular illumination," *Appl. Opt.*, vol. 51, no. 13, pp. 2257–2263, May 2012, doi: 10.1364/AO.51.002257.

[9] R. Wu *et al.*, "Design of freeform illumination optics," *Laser Photon. Rev.,* vol. 12, no. 7, May 2018, doi: 10.1002/lpor.201700310.

[10] J. Zheng and K. Qian, "Designing single LED illumination distribution for direct-type backlight," *Appl. Opt.*, vol. 52, no. 28, pp. 7022–7027, Oct. 2013, doi: 10.1364/AO.52.007022.

[11] J. Muschaweck, "Optoelectronic component and illumination device," U.S. Patent 8 672 500 B2, vol. 18, Mar. 2014.

[12] K. Wang, Y. J. Han, H. T. Li, and Y. Luo, "Overlapping-based optical freeform surface construction for extended lighting source," *Opt. Exp.*, vol. 21, no. 17, pp. 19750–19761, Aug. 2013, doi: 10.1364/OE.21.019750.

[13] Y. Luo, Z. Feng, Y. Han, and H. Li, "Design of compact and smooth free-form optical system with uniform illuminance for LED source," *Opt. Exp.*, vol. 18, no. 9, pp. 9055–9063, Apr. 2010, doi:10.1364/OE.18.009055.

[14] J. Bortz and N. Shatz, "Iterative generalized functional method of nonimaging optical design," in *Proc. SPIE*, 2007, pp. pp.66700A-1–66700A-15, doi: 10.1117/12.731897.

[15] W. J. Cassarly, "Iterative reflector design using a cumulative flux compensation approach," in *Proc. SPIE*, 2010, pp. 76522L-1–76522L-9, doi: 10.1117/12.871698.
[16] W. Situ, Y. Han, H. Li, and Y. Luo, "Combined feedback method for designing a free-form optical system with complicated illumination patterns for an extended LED source," *Opt. Exp.*, vol. 19, no. S5, pp. A1022–A1030, Sep. 2011, https://doi.org/10.1364/OE.19.0A1022.
[17] X. Mao, H. Li, Y. Han, and Y. Luo, "Two-step design method for highly compact three-dimensional freeform optical system for LED surface light source," *Opt. Exp.*, vol. 22, no. S6, pp. A1491–A1506, Oct. 2014, doi: 10.1364/OE.22.0A1491.
[18] R. Wu, Y. Qin, H. Hua, Y. Meuret, P. Benítez, and J. C. Minano, "Prescribed intensity design for extended sources in three-dimensional rotational geometry," *Opt. Lett.*, vol. 40, no. 9, pp. 2130–2133, May 2015, doi: 10.1364/OL.40.002130.
[19] Z. Ding *et al.*, "Designing compact and ultra-efficient illumination lenses with prescribed irradiance properties for extended light sources," *Opt. Commun.*, vol. 465, no. 125601, pp. 1–10, Feb. 2020, doi: 10.1016/j.optcom.2020.125601.
[20] 2020. [Online]. Available: http://www.latticepower.com/NewsView.aspx?id=262